Electron Tunneling and Capacitance Studies of a Quantized Surface Accumulation Layer

D. C. Tsui
Bell Laboratories, Murray Hill, New Jersey 07974
(Received 7 March 1973)

This paper presents an experimental study of the effect of surface quantization in an accumulation layer on electrostatic screening. The accumulation layer exists at the InAs surface of an n-type InAs-oxide-Pb junction and is caused by redistribution of carriers to screen out an external electric field at the InAs surface. The results of this study confirm two predictions made by Baraff and Appelbaum. First, the appearance or disappearance of a subband of surface states introduces no sudden change in the surface potential well. Second, the magnetic quantization of the two-dimensional subbands causes oscillations in the surface potential well. We have observed the magneto-oscillations in the surface potential U_0 and in the E_b of the quantum level, which the surface potential well supports. The oscillations in U_0 are observed directly in the magneto-capacitance of the junction. Moreover, these oscillations appear as a modulation to the potential barrier at the InAs-oxide interface and give rise to a new magneto-oscillatory effect in the tunneling characteristics of the InAs-oxide-Pb tunnel junctions. We have observed this new oscillatory effect and utilized it to estimate the bias dependence of E_b. We have also determined the effective cyclotron mass of carriers in the subband, which is approximately 10% heavier than that of carriers in the conduction band.

I. INTRODUCTION

This paper is a continuation of an earlier one dealing with an experimental study of quantum effects in the accumulation layer at an n-type InAs surface. The earlier paper,[1] which will henceforth be referred to as I, described the electron-tunneling experiments, which are performed on n-type InAs-oxide-Pb tunnel junctions, and discussed two results. First, the tunneling curves, i.e., the conductance dI/dV vs applied bias V and the derivative of the conductance d^2I/dV^2 vs V curves, show structures reflecting the energy minima of the two-dimensional electric subbands. The bias position V_b of these structures gives a direct measure of the energy E_b of the quantum levels. Second, when a magnetic field is applied perpendicular to the junction surface, oscillations are observed in these tunneling curves. These oscillations arise from Landau magnetic quantization of the two-dimensional continua of the electric subbands[2] and thus reflect the Landau-level spectra of the surface electrons. It was noted that the applied bias has an effect of making the bias separation between neighboring conductance peaks in the tunneling curves larger than the energy separation of the surface-electron Landau levels. Consequently, it can cause an apparent reduction in the effective cyclotron mass determined from these measurements. A parallel magnetic field induces a shift of the subband energy minimum, which is a measure of the spread of the quantum state.[2,3] Measurements of this shift were given in Ref. 4.

In this paper, we wish to discuss some additional data from the electron-tunneling experiments and the data from a capacitance experiment on InAs-oxide-Pb junctions. We discuss them in terms of the simple physical models given in I and some results of the self-consistent field calculations of Baraff and Appelbaum.[5,6] In Sec. II we determine the effective cyclotron mass of the subband electrons from the Landau-level oscillations in the tunneling curves, taking into account the effect of an applied bias on E_b. The effective cyclotron

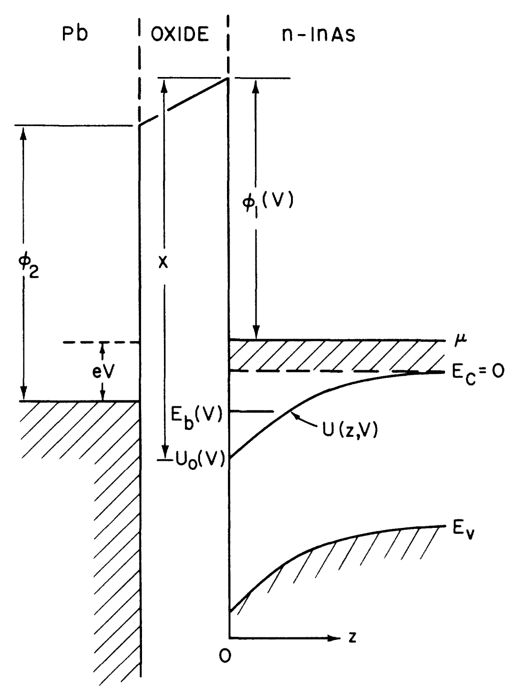

FIG. 1. Energy diagram for an n-type InAs-oxide-Pb junction with a bias V applied to the Pb electrode. The potential well $U(z, V)$ associated with the accumulation layer supports one quantum level at an energy $-E_b(V)$.

mass deduced from our measurements is approximately 10% enhanced over its conduction-band value. Section III describes some new magneto-oscillatory effects in electron tunneling, which arise from the oscillations in the surface potential well when the electric subband is quantized into Landau levels. In Sec. III A we discuss the oscillatory effect which reflects the oscillations in U_0, the depth of the potential well at the InAs-oxide interface. Oscillations are also observed in E_b vs H curves of some lightly doped samples, which have two quantum levels in the surface potential well. We present the data on magneto-oscillatory effects from these samples in Sec. III B and show that the observed magneto-oscillatory behavior of E_b indeed arises from magnetic quantization of electrons in the electric subbands, as predicted by Baraff and Applebaum's calculations

Section IV describes the capacitance experiment and discusses in detail three pertinent results. First, a quantized accumulation layer of electrons exists at the InAs surface at $V=0$. Second, magneto-oscillations are observed in the capacitance measurements. These oscillations, reflecting the oscillations in U_0, are due to the magnetic quantization of electrons in the two-dimensional subbands. The magnetic quantization of electrons in the conduction band has no observable effect in the capacitance measurements. Third, we have made an experimental test of a result from Baraff and Appelbaum's calculations. This result, which is a special case of the general theorem by Kohn and Majumdar[7] for a system of noninteracting fermions, states that the self-consistent potential varies continuously with the external electric field.

II. EFFECTIVE CYCLOTRON MASS

Figure 1 shows the potential energy diagram of an idealized InAs-oxide-Pb tunnel junction with a bias $V>0$ applied to the Pb electrode. $U(z, V)$ and $E_b(V)$ (measured from E_c) are, respectively, the bias-dependent potential of the accumulation layer and the quantum energy level it supports. The conductance dI/dV due to electrons in the subband[8] is directly proportional to the density of states η_s of the subband at an energy eV away from the Fermi level μ, i.e.,

$$\frac{dI}{dV} \propto \eta_s(\mu - eV). \tag{1}$$

Since η_s of a two-dimensional energy band has a step-function discontinuity at the band edge, a decrease in the dI/dV-vs-V curve occurs at eV equal to the energy of a quantum level measured from μ. This subband-band-edge effect appears as a dip in the d^2I/dV^2-vs-V curve. The bias position V_b of this dip measures E_b when V_b is applied to the junction, i.e.,

$$eV_b = \mu + E_b(V_b). \tag{2}$$

When a magnetic field H is applied perpendicular to the plane of the junction, it quantizes the two-dimensional subband into discrete Landau levels. If we neglect level broadening, η_s is split into a series of δ-function peaks at the energy of the Landau levels. The dI/dV-vs-V curve, which reflects η_s directly, shows oscillations reflecting the energy structure of the Landau levels. The dI/dV peaks occur at biases satisfying

$$eV = \mu + E_b(V) - \epsilon_n(H), \tag{3}$$

where $\epsilon_n(H)$ is the energy of the nth Landau level measured from $E_b(V)$. In the bias range of interest, we may assume a linear dependence of E_b on V and write

$$E_b(V) = E_b(V_b) + \gamma e(V - V_b), \tag{4}$$

where γ is a positive constant, which can be determined from additional experimental data to be discussed in detail in Sec. III A. We believe that this assumption is valid for two reasons: (i) Baraff and Appelbaum have made numerical calculations for E_b and the surface potential U_0 as a function of the total screening charge Q in the InAs electrode. In the range of Q pertinent to our experiments, i.e., $1\times10^{12} \lesssim Q \lesssim 3\times10^{12}/\text{cm}^2$, both E_b and U_0 show an approximately linear dependence on Q. This implies that E_b depends approximately linearly on V. (ii) We have observed additional oscillatory effects which arise from the bias dependence of E_b. As discussed in Sec. III A, these additional data can be quantitatively explained by this assumption. From Eqs. (2)–(4), we obtain that the conductance peak reflecting the nth Landau level in the subband occurs at a bias

$$V_n^L(H) = V_b - \epsilon_n(H)/(1-\gamma)e. \tag{5}$$

The effective cyclotron mass defined by

$$m_n^*(H) = \frac{\hbar e H}{c}\,[\epsilon_{n+1}(H) - \epsilon_n(H)]^{-1} \tag{6}$$

can be determined from measuring the bias separation between two neighboring conductance peaks using

$$m_n^*(H) = \frac{\hbar H}{(1-\gamma)c}\,[V_n^L(H) - V_{n+1}^L(H)]^{-1}. \tag{7}$$

Figure 2 shows m_n^* of subband electrons for $n=0$, 1, and 2, deduced from our tunneling data using Eq. (7), as a function H. The data were obtained from sample 57894 (crosses in Fig. 2) and from sample 57891 (triangles in Fig. 2) of I. Both samples have one quantized energy level in the potential well of the InAs surface accumulation layer, being observed at $V_b = 168$ mV in sample 57894 and at $V_b = 183$ mV in sample 57891. The constant γ, obtained according to the discussions given in Sec. III A, is 0.18 ± 0.01 for both samples. We note that while the error bar indicates the uncertainties in determining V_n^L, the spread seen in the data results from the presence of phonon-induced structures and additional oscillatory effects in the tunneling curves, which interfere with the Landau-level oscillations. Within these experimental uncertainties, the results obtained from the two samples are in good agreement.

In order to compare these results with those of the conduction-band electrons, we have calculated $m_n^*(H)$ of the conduction-band electrons using their Landau levels described by the Kane model[9]:

$$\epsilon^c(H) = H\frac{e\hbar}{m_0^* c}(n+\tfrac{1}{2})\frac{\epsilon_g(\epsilon_g+\lambda)}{3\epsilon_g+2\lambda} \times\left(\frac{2}{\epsilon_n^c+\epsilon_g}+\frac{1}{\epsilon_n^c+\epsilon_g+\lambda}\right), \quad (8)$$

where ϵ_g, λ, and m_0^* are the direct-energy gap, the spin-orbit gap, and the band-edge effective mass, respectively. We use $\epsilon_g = 0.41$ eV, $\lambda = 0.38$ eV,[10] and $m_0^* = 0.0215 m_0$,[11] and the results for $n = 0$, 1, and 2 are shown as solid curves in Fig. 2.

It is clear that the effective cyclotron mass of electrons in the subband is approximately 10% enhanced over its conduction-band value. Similar mass enhancement has been observed in the surface inversion layer of p-type $Hg_{0.79}Cd_{0.21}Te$ by Antcliffe, Bate, and Reynolds.[12] They demonstrated, by a quasiclassical calculation, that this mass enhancement can result directly from the surface quantization of a nonparabolic energy band. More recently, Smith and Stiles[13] observed mass enhancement as a function of the carrier concentration in an n-inversion layer of Si. Their results are attributed to electron-electron interactions. Since the conduction band of InAs is nonparabolic, the mass enhancement demonstrated by Antcliffe *et al.* is expected. A quantitative account of this experimental result must await a proper self-consistent treatment of the accumulation layer which takes into account the conduction-band nonparabolicity.

III. SURFACE POTENTIAL WELL

In this section and in Sec. IV, we discribe some experimental results concerning the effect of the quantization of a surface accumulation layer on the electrostatic screening by carriers near the surface of a semiconductor. This effect has been investigated by Baraff and Appelbaum in their self-consistent field calculations. In order to present some of their results, we recall that the potential well $U(z)$ is the energy of an electron in the electrostatic potential $u(z)$, which is determined by the charge distribution in the semiconductor through the Poisson equation:

$$U(z) = -eu(z), \quad (9a)$$

$$\frac{d^2u(z)}{dz^2} = -(4\pi/\kappa)\rho(z), \quad (9b)$$

with boundary conditions

$$u(z=\infty) = 0, \quad (10)$$

$$\left.\frac{-du(z)}{dz}\right|_{z=0} = F_0. \quad (11)$$

Here, κ is the state dielectric constant of the semiconductor; F_0 is the electric field at its surface $z = 0$ related to the total screening charge Q in the semiconductor through

$$Q = \int_0^\infty \rho(z)dz = -(\kappa/4\pi)F_0; \quad (12)$$

$\rho(z)$ is the charge density given by the bulk conduction electrons, surface subband electrons, and the ionized donors. In their parametric approach, Baraff and Appelbaum assumed an approximate

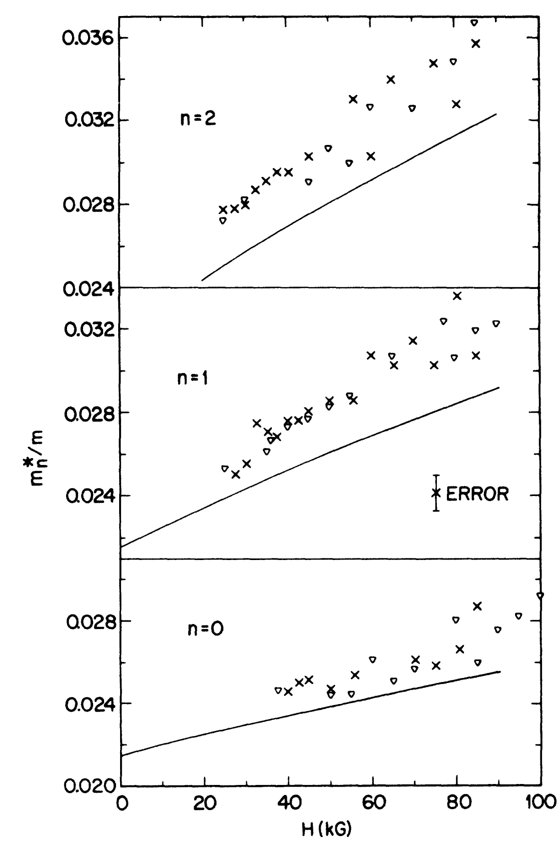

FIG. 2. m_n^* of the subband for $n = 0$, 1, and 2 as a function of perpendicular H. The crosses ($\times$) and the triangles (∇) are deduced from the tunneling data on samples 57894 and 57891 of I, respectively. The solid curves show m_n^* of the conduction band.

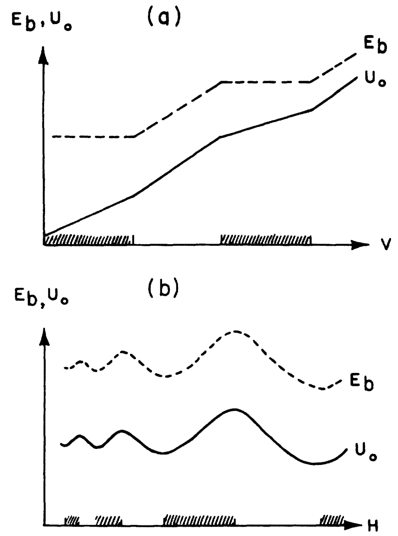

FIG. 3. Schematic illustration of the magneto-oscillatory behavior of E_b and U_0 (a) at constant H and (b) at constant V. A Landau level of the subband is pinned to the Fermi level in the shaded regions of V and H.

form for the potential energy,

$$U(z) = \frac{-U_0}{1-\beta}\,(e^{-\lambda z} - \beta e^{-2\lambda z}) \tag{13}$$

and solved the Schrödinger equation, the equation for charge density, and the Poisson equation exactly. Self-consistency is achieved by demanding that the boundary condition in Eq. (11) is satisfied, that the computed screening charge equals that given by the electric field at the semiconductor surface through Eq. (12), and that the resulting potential at $z=0$ agrees with the starting potential at $z=0$. The two parameters U_0 and λ in Eq. (13) measure the potential well at $z=0$ and the range of the potential, respectively. The third parameter β can be expressed in terms of U_0 and λ through the boundary condition on $u(z)$ expressed by Eq. (11).

Two of their predictions are most important to the understanding of our data. First, the self-consistent potential varies continuously with the electric field F_0. The appearance or disappearance of a subband of surface electrons introduces no sudden change in the screening properties of the semiconductor. Second, the magnetic quantization of the two-dimensional subbands causes magneto-oscillations in the self-consistent potential. The magnetic quantization of the bulk conduction electrons has no observable contribution to this oscillatory behavior. The first prediction has been confirmed experimentally by the use of capacitance measurements on InAs-oxide-Pb junctions, to be discussed in Sec. IV. In the rest of this section, we shall recapitulate the magneto-oscillatory behavior of U_0 and E_b as predicted by Baraff and Appelbaum and relate it to the additional oscillatory effects observed in our electron-tunneling experiment. The magneto-oscillations in U_0 also cause oscillations in the magnetocapacitance of an InAs-oxide-Pb junction. Discussions of such oscillatory effects in the magnetocapacitance are given in Sec. IV.

Figure 3 illustrates qualitatively the oscillatory behavior of E_b and U_0. If H is fixed, both E_b and U_0 must increase with increasing V to accommodate the additional electrons required to screen out the electric field from V. However, when a surface Landau level (either to be filled or to be emptied) is pinned to the Fermi level, E_b cannot change with V. As a result, E_b remains constant and the rate of change of U_0 with respect to V assumes a smaller value during the pinning of a Landau level to the Fermi level. This causes the steplike behavior of E_b and U_0 seen in Fig. 3(a). On the other hand, if V is kept fixed, the total screening charge remains constant. When a surface Landau level is pinned to the Fermi level, the increase in the Landau-level energy with increasing H must be compensated by an increase in E_b, which in turn demands an increase in U_0, Consequently, as H increases, E_b and U_0 increase during the pinning of a Landau level and decrease while there is no Landau level pinned to the Fermi level. This is the origin of the de Haas–van Alphen-type oscillations in the E_b and U_0 vs H plots illustrated in Fig. 3(b).

The oscillatory behavior in U_0 appears as a modulation on the oxide barrier height and gives rise to a new magneto-oscillatory effect in tunneling. We shall describe in Sec. III A the data obtained from sample 57894 of I and utilize these data to determine the constant γ in Eq. (4). The oscillatory behavior in E_b has been observed in the E_b vs H data of less heavily doped samples, which have two quantum levels. We shall describe this result in Sec. III B, together with the Landau-level data on these less heavily doped samples.

A. Magneto-Oscillations in U_0

As seen in Fig. 1, the barrier height at $z=0$, seen by electrons at the InAs Fermi level, is given by

$$\phi_1(V) = \chi - [U_0(V) + \mu], \tag{14}$$

where χ is the electron affinity at the InAs-oxide interface.[14] Since both χ and μ are fixed, an increase (or decrease) in U_0 with increasing V or H will decrease (or increase) ϕ_1. This decrease (or increase) in ϕ_1 in turn will enhance (or suppress) the tunneling probability of the bulk conduction states and cause an increase (or decrease) in

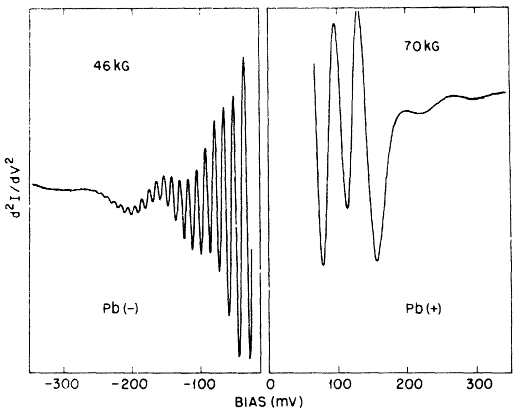

FIG. 4. d^2I/dV^2-vs-V curves from sample 57894 of I at $T = 4.2$ °K. The magnetic field is applied perpendicular to the junction surface and the bias is the voltage applied to the Pb electrode.

the tunnel conductance. Therefore, the magneto-oscillations in U_0 can cause new oscillatory effects in the tunneling characteristics of the junction.

Figure 4 shows the experimental data on this magneto-oscillatory effect in the d^2I/dV^2-vs-V curves taken from sample 57894 of I at 4.2 °K. The dominant short-period oscillations seen in Fig. 4 consist of two sets: One, shown in the left-hand side panel, reflects the Landau levels of the bulk conduction electrons; the other, shown in the right-hand side panel at $V \lesssim 168$ mV, reflects the Landau levels of the surface electrons. We have used an ac modulation signal, which overmodulated these Landau-level oscillations, to enhance the new oscillations which have a longer period. These new oscillations are better resolved at large biases and are most clearly seen in the bias range $V > 168$ mV, in which no Landau-level oscillations exist. Figure 5 shows this new oscillatory effect in two d^2I/dV^2-vs-H curves taken at constant V. These oscillations are periodic in $1/H$. At $V = -240$ mV, the period of the new oscillations is approximately five times as long as the Landau-level oscillations. At $V = +250$ mV, the Fermi level of the Pb electrode lies below the subband minimum ($V_b = 168$ mV). The Landau-level oscillations, which reflect the passing of the Landau levels of the subband across the Fermi level of Pb, cannot exist. The new oscillations, on the other hand, reflect the passing of the Landau levels of the subband across the Fermi level of the InAs electrode. They are resolved at $H \gtrsim 50$ kG. The other set of oscillations, which will be discussed

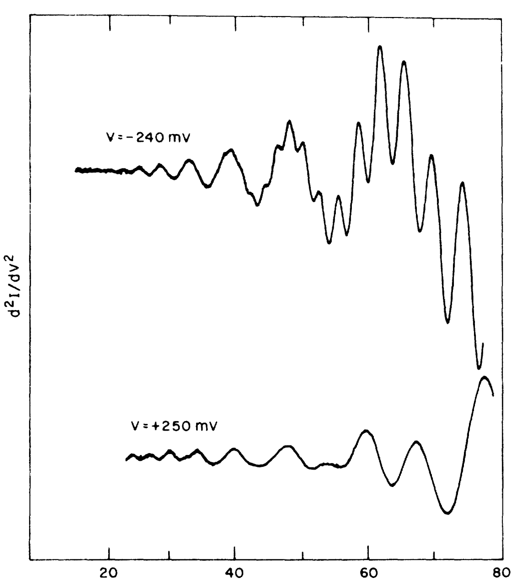

FIG. 5. d^2I/dV^2-vs-H curves at constant V from sample 57894 of I at $T = 4.2$ °K.

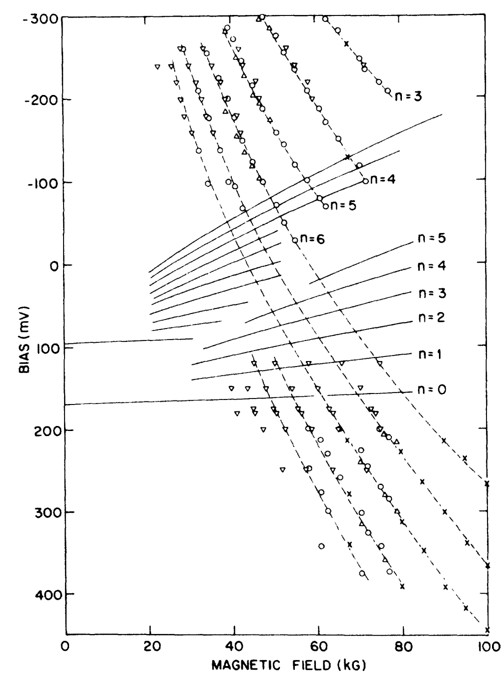

FIG. 6. Summary of the magneto-oscillation data from sample 57894 of I. The data on the new magneto-oscillatory effect discussed in the text are shown as points: the circles (○), the upright triangles (△), and the crosses (×) show the bias position of oscillation dips in the d^2I/dV^2-vs-V curves taken at constant H and the inverted triangles (▽) show the peaks in the d^2I/dV^2-vs-H curves taken at constant V. The two sets of solid curves show the bias position of d^2I/dV^2 dips in the Landau-level oscillations of the electrons and the conduction-band electrons. The value of n is the quantum number of the Landau level which causes the observed structure in the d^2I/dV^2 curves.

in more detail at the end of this subsection, reflect the Landau-level oscillations of the conduction band. We have also verified that this new oscillatory effect depends only on the perpendicular component of an arbitrarily oriented magnetic field, consistent with its having an origin in the magnetic quantization of the surface electrons.

Figure 6 summarizes the magneto-oscillation data of sample 57894. The circles and the crosses show the bias position of oscillation dips in the d^2I/dV^2-vs-V curves as a function of the perpendicular magnetic field. For the crosses, the applied magnetic field is kept constant at 100 kG, and the various values of the perpendicular magnetic field are obtained by varying the field orientation. The triangles show the magnetic field position of peaks in the d^2I/dV^2-vs-H curves taken at constant V. We note two unusual features here. First, the bias and the magnetic field, which specify a dip in the d^2I/dV^2-vs-V curve, specify a peak in the d^2I/dV^2-vs-H curve. This results from the difference in the dependence of U_0 on V and the dependence of U_0 on H, as illustrated in Fig. 3. For example, during the pinning of a Landau level to the Fermi level, U_0 increases with increasing H. On the contrary, U_0 decreases its slope with increasing V during this pinning. In a U_0 vs V plot, this behavior of U_0 appears as a periodic decrease superposed on an increasing background. Second, the slope of the dashed curves drawn through our data points is negative, opposite to that of the two sets of solid curves which indicate that d^2I/dV^2 dips in the Landau-level oscillations of the surface electrons and the bulk conduction electrons. This difference follows from our model in that an oscillation due to the barrier modulation effect appears each time a Landau level in the subband of InAs moves through the Fermi level of the InAs electrode, while, on the other hand, a Landau-level oscillation appears whenever a Landau level of InAs passes by the Fermi level of the Pb electrode.

If H is kept constant, whenever V satisfies

$$\mu + E_b(V) = \epsilon\ (H), \tag{15}$$

a Landau level in the subband is aligned with the Fermi level of the InAs electrode and the barrier modulation effect causes a dip in the d^2I/dV^2-vs-V curve. Assuming that V_b depends linearly on V, we obtain by combining Eqs. (2), (4), and (15) that the bias, at which d^2I/dV^2-vs-V shows a dip due to the pinning of the nth surface Landau level, is given by

$$V_n^M(H) = V_b(1 - 1/\gamma) + \epsilon_n(H)/\gamma e. \tag{16}$$

Obviously, if we plot V_n^M as a function of H, the sign for the slope of the resulting curves is opposite to that for V_n^L as a function of H given by Eq. (5). In the limit $H \to 0$, all the curves converge onto the bias $V_n^M(0) = V_b(1 - 1/\gamma)$. Since V_b is known from the zero-field measurements, we can determine γ from these oscillatory data directly. For sample 57894, we obtain $V_n^M(0) = 750 \pm 50$ mV by extrapolating the dashed curves in Fig. 6 to $H = 0$. This yields $\gamma = 0.18 \pm 0.01$. On the other hand, from Eq. (5) and Eq. (11), V_n^L and V_n^M corresponding to the same Landau level of the subband are related by

$$V_n^M(H) = (1 - 1/\gamma) V_n^L(H). \tag{17}$$

Our data on V_n^M and V_n^L, as shown in Fig. 6, can be described by Eq. (17) with $\gamma = 0.180 \pm 0.015$.

At constant V, these new oscillations in d^2I/dV^2 are periodic in $1/H$. This is demonstrated in Fig. 7 by plotting the inverse magnetic field, at which the d^2I/dV^2 peaks are observed, as a function of the peak number. The period $P(V)$ of the oscillations is the slope of the resulting straight line. Since the applied magnetic field causes only small-amplitude oscillations in E_b, which are not observed in these samples, $P(V)$ is a measure of the area in the (k_x, k_y) plane enclosed by the Fermi-energy contour.[15] The surface-electron density $N_s(V)$ at V, which is equal to the total number of states contained inside this constant-energy contour, is given by

$$N_s(V) = \frac{e/\pi\hbar c}{P(V)}\ . \tag{18}$$

Figure 8 shows $N_s(V)$ deduced from our measurements on sample 57894. The surface electron density at $V = +168$ mV, the bias applied to measure the energy of the quantum level, is $N_s(V_b)$

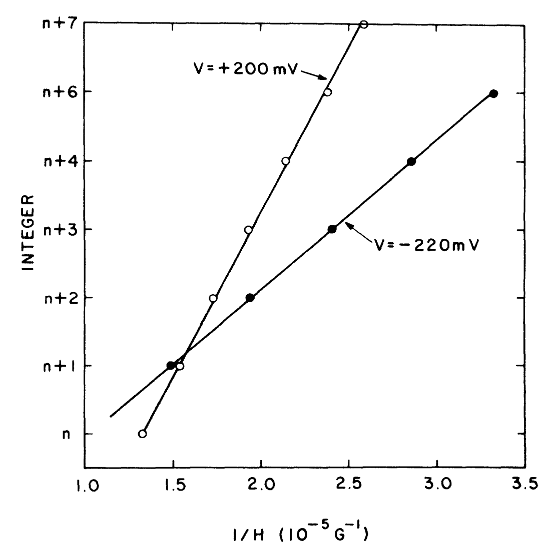

FIG. 7. Plots of the oscillation number vs $1/H$ obtained from d^2I/dV^2-vs-H curves.

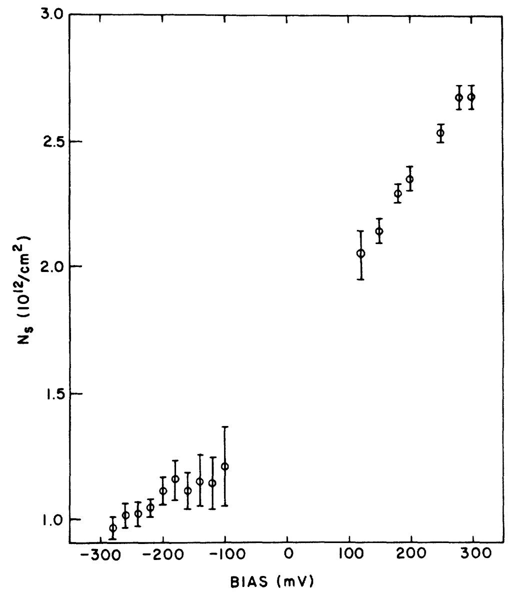

FIG. 8. N_s-vs-V deduced from sample 57894 of I.

$=2.2\times10^{12}/\mathrm{cm}^2$. An interpolation of the data to zero bias yields $N_s(0)\approx 1.7\times10^{12}/\mathrm{cm}^2$, which agrees with the value deduced from the surface Landau-level oscillations given in I.

For $V \gtrsim 150$ mV, another set of oscillations are observed in the d^2I/dV^2-vs-H curves. This is most clearly seen in Fig. 5, where, for $V=+250$ mV, the oscillations due to the barrier modulation effect are resolved at magnetic fields $H \gtrsim 50$ kG. The other set of oscillations, which are more visible at smaller H, are not observed in either the d^2I/dV^2-vs-V curves or the d^2I/dV^2-vs-H curves with $V<0$. The period of the oscillations shows no bias dependence and is equal to the period of the bulk-conduction-electron Landau-level oscillations at zero bias. These observations suggest the following explanation[16]: When a bulk-conduction-band Landau level moves through the Fermi level of the InAs electrode, it causes a sudden increase in the electron-tunneling probability at the Fermi level. This gives rise to an oscillatory effect in the tunneling characteristics as a function of H at $V>0$. This effect is negligible for $V<0$ and does not exist if H is kept constant.

B. Magneto-Oscillations in E_b

Since V_b measures E_b directly through Eq. (2), we shall use V_b and E_b interchangeably in discussing the magneto-oscillations in E_b. These oscillations have been observed in all the less heavily doped samples ($n \lesssim 1.5\times10^{17}/\mathrm{cm}^3$), which have two quantum levels in the surface accumulation layer. However, some of these junctions show a positive magnetoresistance,[17(a)] which is the least heavily doped samples ($n\approx 2\times10^{16}/\mathrm{cm}^3$) at $H\approx 40$ kG can be as large as twice their zero-field tunnel resistance. Since the origin of this magnetoresistance is still unknown, we do not discuss the oscillations in V_b from these samples. We shall discuss the data typical of tunnel junctions which do not exhibit magnetoresistance and show that, in this case, there is conclusive evidence that the oscillatory behavior of V_b indeed arises from magnetic quantization of the subbands, as predicted by the calculations of Baraff and Appelbaum.

Figure 9 shows the effect of a quantizing magnetic field on the d^2I/dV^2-vs-V curves of an InAs-oxide-Pb junction (TJ137), whose InAs electrode has $n=1.3\times10^{17}/\mathrm{cm}^3$. These data were taken at 4.2 °K. The uppermost curve is taken with the minimum magnetic field necessary to quench the superconductivity of the Pb electrode. As discussed previously,[17(b)] the structures near zero bias ($|V| \lesssim 30$ mV) are due to emission and self-energy effects of Pb phonons and InAs phonons. The weak structure at $V_c=45$ mV reflects the conduction-band minimum and measures μ of electrons in the conduction band. The two quantum levels in the surface accumulation layer are observed at $V_{b1}=+70$ mV and $V_{b2}=+192$ mV. The second curve from the top illustrates the effect of a parallel magnetic field (i.e., $\vec{H}\perp\vec{I}$) which does

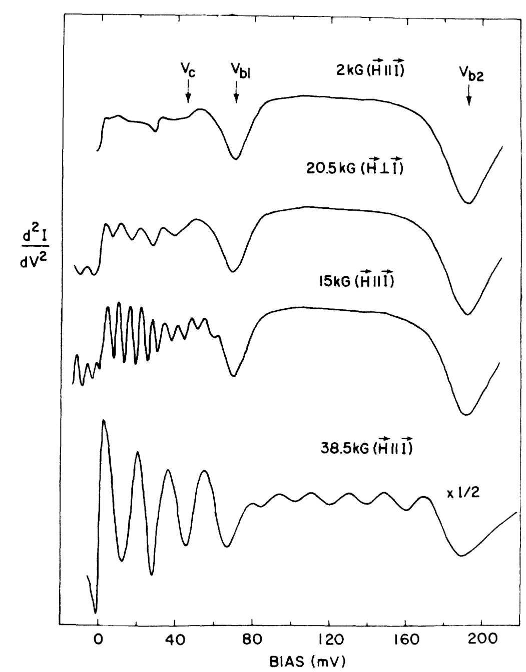

FIG. 9. d^2I/dV^2-vs-V curves of an n-type InAs ($n=1.3\times10^{17}$/cm)-oxide-Pb junction TJ137. V_c indicates the conduction-band minimum; V_{b1} and V_{b2} indicate the excited-state and the ground-state quantum levels, respectively.

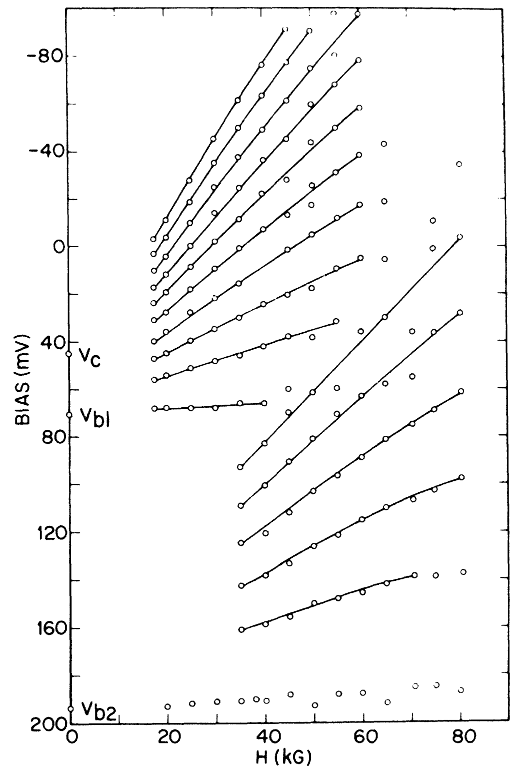

FIG. 10. Summary of data on the Landau-level oscillations of the two subbands of sample TJ137 by plotting the bias position of dips in the d^2I/dV^2 oscillations as a function of perpendicular H.

not quantize the subbands. In this field orientation, Landau-level oscillations are observed at $V \lesssim +45$ mV. They arise from magnetic quantization of the conduction band. On the other hand, when the magnetic field is applied perpendicular to the surface (i.e., $\vec{H} \parallel \vec{I}$), Landau-level oscillations of both subbands are observable. This is shown in the lower two curves of Fig. 9; the oscillations due to magnetic quantization of the two subbands are seen at $V \lesssim V_{b2}$. An unusual result from these data is that, while the oscillations of the excited-state subband (V_{b1}) are observable at $H \gtrsim 13$ kG, those of the ground-state subband (V_{b2}) are not observable until $H \gtrsim 30$ kG. The scattering time of electrons in the excited subband is therefore ≈ 2.3 times that of electrons in the ground-state subband. This difference in scattering time, which also appears in the oscillatory magnetocapacitance data (Sec. IV), is understandable if we recall that the wave function of the excited state extends deeper into the bulk sample than that of the ground state. Consequently, electrons in the excited subband are less sensitive to surface scattering. In other words, since electrons in the ground-state subband are confined to move in a thinner layer on the surface, they are more easily scattered by surface imperfections.

In Fig. 10 we summarize the data on Landau-level oscillations of the two subbands by plotting the bias position of dips in the d^2I/dV^2 oscillations as a function of the perpendicular magnetic field. It is apparent that the data points group themselves into two sets of curves, each reflecting the Landau-level spectra of a subband. In the zero-field limit, the set reflecting Landau levels of the excited subband can be extrapolated to converge onto V_{b1} and the other set onto V_{b2}. As discussed previously, the period of the oscillations in d^2I/dV^2-vs-H curves at constant V is a direct measure of the surface electron density at V. From these data, we have obtained that at zero bias the density of surface electrons is $N_{s1} = 7.7 \times 10^{11}/\mathrm{cm}^2$ in the excited-state subband and $N_{s2} = 2.0 \times 10^{12}/\mathrm{cm}^2$ in the ground-state subband.

It can also be seen in Fig. 10 that V_{b2}, the bias at which the ground-state subband edge is observed, shows magneto-oscillatory behavior. The evidence that this oscillatory effect indeed arises from magnetic quantization of the subbands is seen in Fig. 11 which compares it with the magneto-oscillatory conductance of this junction at $V = +200$ mV. At this bias, the oscillations in the tunnel conductance result from oscillations in the surface potential U_0 which appears as a modulation of the effective tunnel barrier. As discussed in Sec. III A, this oscillatory behavior is a consequence of magnetic quantization of the subbands. Each of the two sets of magnetoconductance oscillations seen in Fig. 11 corresponds to the passing of Landau levels in one subband through the Fermi level of the InAs electode. The period of these

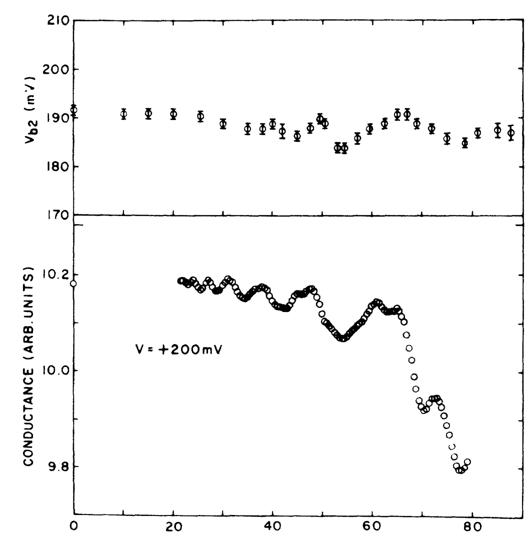

FIG. 11. V_{b2}-vs-H and conductance-vs-H curves of sample TJ137.

oscillations yields $N_{s1} = 1.0\times10^{12}/\mathrm{cm}^2$ and $N_{s2} = 3.3\times10^{12}/\mathrm{cm}^2$ at $V = +200$ mV. We should recall that an increase in U_0 causes an increase in the tunnel conductance. Consequently, since the magneto-oscillations in E_b and those in U_0 are in phase (Fig. 3), we expect that the magneto-oscillations of V_b to be also in phase with these magnetoconductance oscillations. In Fig. 11, only one set of oscillations is apparent in the V_{b2}-vs-H plot. However, its being in phase with the long-period magnetoconductance oscillations is conclusive evidence that this oscillatory effect arises from the magnetic quantization of the excited-state subband. The magnetic quantization of the ground-state subband is expected to cause oscillations having a shorter period. Such oscillations are not resolved in our data. In the case of V_{b1}, interference by the oscillations from the Landau levels of the ground-state subband has made it difficult to resolve any oscillatory effect in our V_{b1}-vs-H data.

IV. MAGNETOCAPACITANCE

The differential capacitance C of an InAs-oxide-Pb junction can be considered as that of two capacitors connected in series, i.e.,

$$C = \frac{dQ}{dV}, \tag{19a}$$

$$1/C = 1/C_0 + 1/C_s. \tag{19b}$$

Here, C_0 is the capacitance of the oxide and C_s is the capacitance of the surface accumulation layer given by

$$C_s = e\,\frac{dQ}{dU_0}. \tag{20}$$

Combining Eqs. (19) and (20), we obtain

$$C = C_0\left(1 - \frac{1}{e}\frac{dU_0}{dV}\right)$$

and

$$\frac{dC}{dV} = -\frac{C_0}{e}\frac{d^2U_0}{dV^2}. \tag{21}$$

It is clear that the magneto-oscillatory behavior of U_0 discussed in Sec. III can cause oscillatory effects in the capacitance of the junction.[18] These oscillatory effects have been observed in the magnetocapacitance measurements on InAs-oxide-Pb junctions at 4.2 °K. In this section we describe these measurements and relate them to the electronic structure of the accumulation layer at the InAs surface.

The measurement of C and dC/dV as a function of V and as a function of H is facilitated by the use of a standard voltage-modulation method. This method, which has been discussed in detail by Amelio,[19] consists of applying an ac modulation voltage to the capacitor and detecting the current flowing through it using a phase sensitive detector. The circuit used in this work is shown in Fig. 12. Briefly, if the voltage applied to the capacitor is

$$V = V_0 + V_1 \sin\omega t, \tag{22}$$

where V_0 is the dc voltage and V_1 is the amplitude of the modulation at a frequency $\omega/2\pi$, the charge stored on the capacitor is

$$Q(V) = Q(V_0) + \left.\frac{dQ}{dV}\right|_{V_0} V_1 \sin\omega t + \frac{1}{2}\left.\frac{d^2Q}{dV^2}\right|_{V_0} (V_1 \sin\omega t)^2 + \cdots. \tag{23}$$

The current is therefore

$$I(V) = \frac{dQ}{dt} = C(V_0)\omega V_1 \cos\omega t + \left.\frac{dC}{dV}\right|_{V_0} \tfrac{1}{2} V_1^2\omega \sin 2\omega t + \cdots. \tag{24}$$

If the current-sensing resistor R_s is made negligible in comparison with the impedance of the capacitor, C is measured directly by detecting the ac signal across R_s at the fundamental frequency $\omega/2\pi$, 90° out of phase with the applied modulation. The second-harmonic signal in phase with the modulation measures dC/dV. If the capacitor is shunted by a resistor R, which is the case of a real semiconductor-oxide-metal structure, the measurement is still reliable if the conductance through the shunted path is negligible in comparison with the capacitive conductance. This requirement and the requirement of a small R_s are conveniently expressed by the following condition:

$$(\omega C R_s)^2 \ll 1 \ll (\omega C R)^2, \tag{25}$$

which can be met by properly choosing ω and R_s. The results discussed in this section are obtained from measurements made under the conditons $\omega CR \gtrsim 100$ and $\omega CR_s \lesssim 0.01$.

The junctions, on which the capacitance measurements are made, are prepared in the same way as the InAs-oxide-Pb tunnel junctions dis-

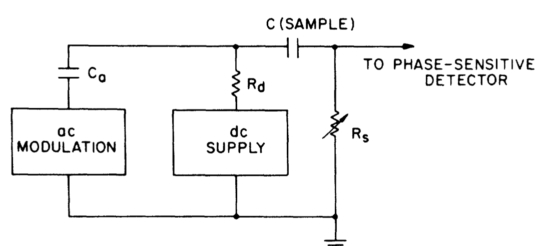

FIG. 12. Schematic representation of the basic circuit for C-V and dC/dV-V measurements.

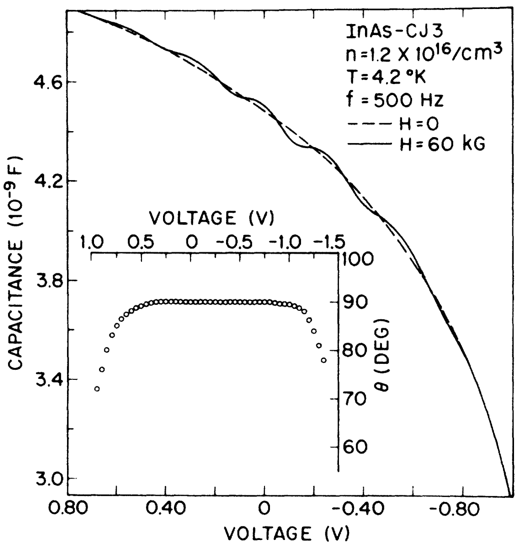

FIG. 13. C-V characteristics of an InAs-oxide-Pb junction at $T=4.2$ °K and $f=500$ Hz. The area of the junction is: $A=(5.34\pm0.1)\times10^{-3}$ cm^2. The insert shows the voltage dependence of the phase angle θ between the signal at the fundamental frequency across R_s and the applied ac modulation.

cussed in I. The oxidation, however, is carried out in a wet oxygen atmosphere for approximately 48 h in order to obtain an oxide thick enough for our capacitance measurements. The oxide prepared in this way is sufficiently thick so that no appreciable electron tunneling is detected with an applied voltage $|V|\lesssim 1$ V. It appears that letting the oxidation continue beyond 48 h does not increase the oxide thickness.

Figure 13 shows the C-V characteristics of an InAs-oxide-Pb junction (area equal to 5.34×10^{-3} cm^2) at 4.2 °K and at 500 Hz. The junction is fabricated on an InAs sample having $n=1.2\times10^{16}$/cm^3. The dashed curve is taken at $H=0$; the solid curve is taken with $H=60$ kG applied perpendicular to the surface. In the frequency range 100 Hz to 1 MHz which we have studied,[20] these C-V curves are frequency independent. A comparison of the voltage dependence seen in the dashed curve with the ideal C-V characteristic of a metal-insulator-semiconductor structure[21] shows that the InAs surface is accumulated in most of this voltage range. For large voltages ($|V|\gtrsim 1$ eV), the conductance due to electron tunneling through the oxide becomes appreciable and the capacitance measurement becomes unreliable. This is seen in the insert of Fig. 13, which shows the voltage dependence of the phase angle θ between the signal at the fundamental frequency across R_s and the applied ac modulation. Deviations of θ from 90° are indicative of tunnel current flowing through the oxide. The abrupt change of θ observed at $V\approx-1.1$ V and at $V\approx+0.7$ V may be attributed to the onset of tunnel current when V equals approximately the height of the potential barriers ϕ_1 and ϕ_2 at the two interfaces of the InAs-oxide-Pb structure (Fig. 1). The potential barrier obtained from this measurement is approximately 1.1 eV at the InAs-oxide interface and approximately 0.7 eV at the oxide-Pb interface. The sign of the bulit-in voltage of the oxide, given by $\phi_1-\phi_2\approx+0.4$ eV, is consistent with the existence of an accumulation layer at the InAs surface in the absence of any external voltage. We have measured the junction capacitance to $V=+1$ V using a capacitance bridge and observed that the capacitance begins to show the expected saturation behavior when the InAs surface is so accumulated that $C_s \gg C_0$ and the junction capacitance approaches C_0. By extrapolating our C-V curve to its saturation, we obtain $C_0\approx9.2\times10^{-7}$ F/cm^2. This yields an average oxide thickness $t_a\approx10\kappa_0$ Å and an average electric field $F_a\approx(4/\kappa_0)\times10^6$ V/cm in the oxide Unfortunately, we have not been able to determine κ_0, the oxide dielectric constant. From the fact that no tunnel current flows near $V\approx0$, we may infer that $t_a>20$ Å and $\kappa_0>2$.

The solid curve in Fig. 13 shows the oscillations in the C-V characteristic when a magnetic field is applied perpendicular to the junction. These oscillations depend only on the perpendicular component of an arbitrarily oriented magnetic field, consistent with their being caused by the magnetic quantization of surface electrons.[2] It is apparent from Eq. (21) and from the oscillatory behavior of U_0 as illustrated in Sec. III that the observed capacitance maxima occur whenever a subband Landau level is pinned to the Fermi level μ of the bulk InAs to be either filled or emptied. The period ΔV of these oscillations is the change in V re-

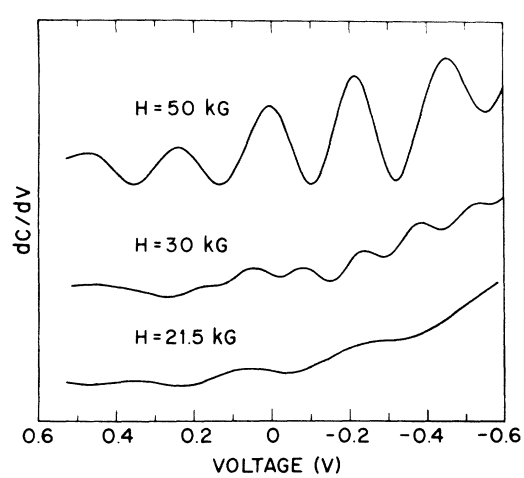

FIG. 14. dC/dV-vs-V curve at constant H from sample CJ3.

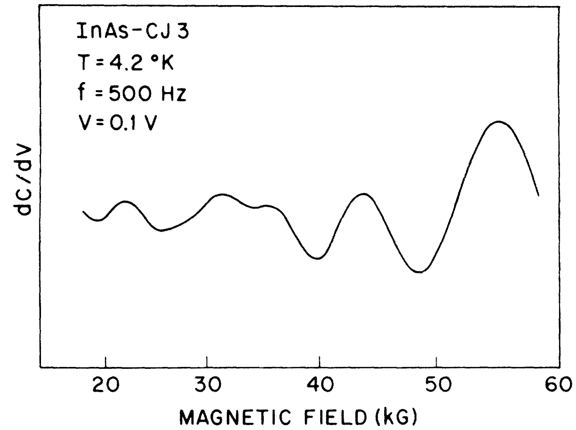

FIG. 15. dC/dV-vs-H curve at constant V. H is applied perpendicular to the surface.

quired to move the subband with respect to μ by $\Delta\epsilon$, the energy separation between two neighboring Landau levels of the subband. Since the change in the screening charge Q is given by

$$\Delta Q = \int C(V)\,dV, \tag{26}$$

we can regard ΔV as a measure of the change in Q required to produce a change of $\Delta\epsilon$ in the binding energy E_b of electrons in the subband. In other words, ΔV measures the slope of the E_b-vs-Q curve of the subband.

Figure 14 shows the dC/dV-vs-V curves for three values of H, which is applied perpendicular to the junction. Figure 15 shows a dC/dV-vs-H curve with $V = +0.1$ V applied to the Pb electrode. It is apparent from these curves that two sets of oscillations are observed, each reflecting the Landau levels of a subband. The existence of two subbands of surface electrons is also observed in the tunneling measurements made on junctions prepared on the same bulk InAs sample. The two subband minima are observed at $V_{b1} \approx +50$ mV and $V_{b2} \approx +170$ mV. However, we must note that the tunnel junctions are prepared by oxidizing the InAs sample in a dry oxygen atmosphere whereas the capacitors are prepared in a wet oxygen atmosphere. Because of this difference in the preparation of the oxide, we make no attempt to correlate the capacitance data with the tunneling data quantitatively.

The oscillations in the dC/dV-vs-H curve, which reflect the passing of Landau levles of a subband across μ at constant V, are periodic in $1/H$. Since the period is a measure of the area in the (k_x, k_y) plane at μ and is related to the number of surface electrons in the subband through Eq. (18), it is obvious that the set of oscillations having the longer period is due to the Landau levels of the excited-state subband. The density of surface-electrons in the absence of an external voltage, obtained from oscillations at $V = 0$, is $N_{s1} = 7.0 \times 10^{11}/\mathrm{cm}^2$ in the excited-state subband and $N_{s2} = 1.2 \times 10^{12}/\mathrm{cm}^2$ in the ground-state subband. In the dC/dV-vs-V curves, the two sets of oscillations are most clearly seen in the magnetic field range $25 \lesssim H \lesssim 50$ kG. For $H \gtrsim 50$ kG, the period ΔV of the oscillations due to Landau levels of the excited subband is so large that it is difficult to observe these oscillations in the voltage range which we have studied. For $H < 25$ kG, the shorter-period oscillations due to Landau levels of the ground-state subband are not resolved. As discussed in Sec. III B, this result is consistent with the notion that an electron in the ground-state subband has a shorter lifetime because of its being more easily scattered by surface imperfections. In the intermediate magnetic field range, we observe that the ratio in ΔV for the two sets of oscillations remains approximately constant and equals approximately 3 to 1. This result indicates that the slope of the E_b-vs-Q plot for the ground state is approximately three times that for the excited state.

Figure 16 shows the magnetic field dependence of the oscillations observed in the dC/dV-vs-V curves. The data points show the voltage at which the capacitance maxima are observed in the oscillations due to Landau levels of the ground-state subband. The solid lines are drawn to indicate that the maxima, resulting from the passing of the same Landau level across μ, fall approximately on a straight line. When these lines are extrap-

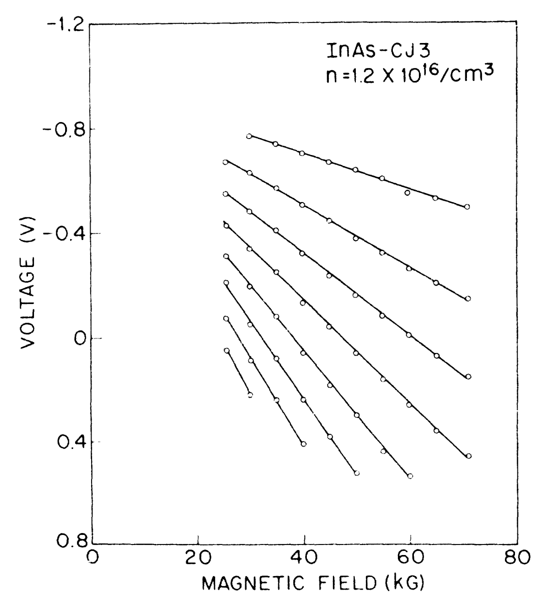

FIG. 16. Capacitance maxima in the dC/dV-vs-V curves of sample CJ3 as a function of the perpendicular magnetic field.

olated to $H=0$, they converge onto a threshold voltage $V_{t2}=-0.97\pm0.02$ V. In the absence of a magnetic field, this is the smallest voltage which must be applied to the Pb electrode to expel the ground-state quantum level from the surface potential well. This corresponds to a change in the screening charge by $\Delta Q=3.3\times10^{12}/\text{cm}^2$. The threshold voltage for the expulsion of the excited level deduced from data on the other set of oscillations is $V_{t1}=-0.85\pm0.02$ V. Having obtained these results, we are able to use the capacitance measurements in the absence of a magnetic field to test one of the results from the calculations of Baraff and Appelbaum. This result, which is a special case of the Kohn-Majumdar[7] theorem for a system of noninteracting fermions, states that the self-consistent potential varies continuously with the external electric field. In terms of this experiment, since μ is finite, the amount of charge stored in the subbands must go through a discontinuity at $V=V_{t1}$ and V_{t2} when a quantum level is expelled from the surface potential well. According to Baraff and Appelbaum, the effect of this discontinuity on the self-consistent potential is canceled by a similar discontinuity in the amount of charge stored in the conduction band. Consequently, no sudden change should result in U_0. Since a kink in the U_0-vs-V curve appears as a step in the C-vs-V curve and as a peak in the dC/dV-vs-V curve, we search for any sudden changes in U_0 by searching for any structure in C and dC/dV-vs-V plots. The fact that we have not found any structure in C-vs-V and dC/dV-vs-V curves at $V\approx V_{t1}$ and V_{t2} can be regarded as an experimental proof of Baraff and Appelbaum's result.

V. CONCLUSIONS

We showed previously[17(b)] that two-dimensional electronic states exist at the InAs surface of an n-type InAs-oxide-Pb junction. These surface states result from the quantization of an accumulation layer, which is caused by the redistribution of electrons near the InAs surface to screen out an electric field. This paper, I, and Ref. 4 together constitute the results of an experimental study of this quantum effect using electron-tunneling measurements and capacitance measurements on n-type InAs-oxide-Pb junctions.[22]

In I and Ref. 4 we discussed three results from electron-tunneling measurements which are pertinent to the energy structure of these surface states. First, the tunneling curves show structures reflecting the energy minima of the two-dimensional subbands. The bias position of the structures gives a measure of the energy of the quantum levels. Second, when a magnetic field is applied perpendicular to the junction surface, oscillations are observed in the tunneling curves. These oscillations, which reflect the Landau-level spectra of the surface electrons, give a measure of their effective mass. Third, when a magnetic field is applied parallel to the junction surface, the energy minimum of the subband is observed to decrease quadratically with an increasing magnetic field. This decrease gives a measure of the spread of the quantum state.

In this paper we have discussed results, from capacitance measurements and from electron-tunneling measurements, which are pertinent to the effect of this surface quantization on the electrostatic screening by carriers near the InAs surface. The results confirm two predictions by Baraff and Appelbaum. First, the appearance or disappearance of a subband of surface electrons does not introduce any sudden change in the surface potential well. Second, the magnetic quantization of the two-dimensional subbands causes oscillations in the surface potential well. We have observed the magneto-oscillations in the surface potential U_0 and the magneto-oscillations in the energy E_b of the quantum level, which the surface potential well supports. The oscillations in U_0 are observed directly in the magnetocapacitance of the junction. Moreover, these oscillations appear as a modulation to the potential barrier at the InAs-oxide-interface and give rise to a new magneto-oscillatory effect in the electron-tunneling characteristics of the InAs-oxide-Pb junctions. We have observed this new oscillatory effect and utilized it to estimate the bias dependence of E_b. We also deduce the effective cyclotron mass of electrons in the subband from the Landau-level oscillations discussed in I, taking into account the bias dependence of E_b. This mass is approximately 10% heavier than that of electrons in the conduction band. The magneto-oscillatory effects, reflecting oscillations in U_0 and E_b, arise from the magnetic quantization of the two-dimensional subbands which depends only on the perpendicular component of an arbitrarily oriented magnetic field. The magnetic quantization of the conduction band has no observable contribution to these oscillatory effects.

Finally, we wish to make two remarks concerning the InAs-oxide-Pb junctions. First, we have obtained no direct information on the origin of the electric field (at the InAs-oxide interface) which causes the accumulation layer at zero bias. Both the work-function difference between the two electrodes[23] and charged defects in the oxides can give rise to this electric field. Unfortunately, we have not succeeded in fabricating tunnel junctions with a metal electrode whose work function is sufficiently different from that of Pb to permit a determination of the effect of the work-function difference. Second, we have no explanation for the anomalous magnetoresistance observed in some of the junctions fabricated on the lightly doped InAs samples. In particular, there is no apparent reason for this magnetoresistance to be observed in some tunnel junctions but not in the others. It appears that further experiments with junctions prepared under better controlled conditions are required to understand this anomaly.

ACKNOWLEDGMENTS

I am most grateful to G. A. Baraff, W. L. McMillan, and J. M. Rowell for their interest and for suggestions and discussions concerning this work, and to G. Kaminsky for technical assistance.

---

[1]D. C. Tsui, Phys. Rev. B **4**, 4438 (1971).

[2]F. Stern and W. E. Howard, Phys. Rev. **163**, 816 (1967).

[3]F. Stern, Phys. Rev. Lett. **21**, 1687 (1968).

[4]D. C. Tsui, Solid State Commun. **9**, 1789 (1971).

[5]G. A. Baraff and J. A. Appelbaum, Phys. Rev. B **5**, 475 (1972); J. A. Appelbaum and G. A. Baraff, Phys. Rev. B **4**, 1235 (1971); Phys. Rev. B **4**, 1246 (1971).

[6]J. A. Appelbaum and G. A. Baraff, Phys. Rev. Lett. **26**, 1432 (1971).

[7]W. Kohn and C. Majumdar, Phys. Rev. **138**, A1617 (1965).

[8]D. J. BenDaniel and C. B. Duke, Phys. Rev. **160**, 679 (1967).

[9]B. Lax, J. G. Mavoorides, H. J. Zeiger, and R. J. Keyes, Phys. Rev. **122**, 31 (1961).

[10]C. R. Pigeon, D. L. Mitchell, and R. N. Brown, Phys. Rev. **154**, 737 (1967); C. R. Pigeon, S. H. Groves, and J. Feinlieb, Solid State Commun. **5**, 677 (1967).

[11]This value of m_0^* is obtained by fitting Eq. (8) to the tunneling data on the conduction-band Landau level spectra of InAs (Ref. 17), using $E_g = 0.41$ eV and $\lambda = 0.38$ eV.

[12]G. A. Antcliffe, R. T. Bate, and R. A. Reynolds, in *The Physics of Semimetals and Narrow Gap Semiconductors*, edited by D. L. Carter and R. T. Bate (Pergamon, New York, 1971), p. 499.

[13]J. L. Smith and P. J. Stiles, Phys. Rev. Lett. **29**, 102 (1972).

[14]See, for example, A. Many, Y. Goldstein, and N. B. Grover, *Semiconductor Surfaces* (North-Holland, Amsterdam, 1965), p. 132.

[15]L. M. Roth and P. N. Argyres, in *Semiconductors and Semimetals*, edited by R. K. Willardson and A. C. Beer (Academic, New York, 1966), Vol. I, Chap. 6.

[16]G. A. Baraff (private communication).

[17](a) D. C. Tsui, Bull. Am. Phys. Soc. **16**, 143 (1971); (b) D. C. Tsui, Phys. Rev. Lett. **24**, 303 (1970); and in *Proceedings of the Tenth International Conference on the Physics of Semiconductors, Cambridge, Mass.*, 1970 edited by S. P. Keller, J. C. Hensel, and F. Stern (U. S. AEC, Oak Ridge, Tenn., 1970), p. 468.

[18]M. Kaplit and J. N. Zemel, Phys. Rev. Lett. **21**, 212 (1968). They first employed magneto-capacitance measurements to study surface quantization of the n-type inversion layer of a Si metal-oxide-semiconductor-field-effect transistor (MOSFET). A detailed analysis of the magneto-capacitance of this device has been given by F. Stern (unpublished) and by A. Voshchenkov (private communication).

[19]G. F. Amelio, Surf. Sci. **29**, 125 (1972).

[20]The C-V characteristic at 1 MHz is measured by using a Boonton rf admittance bridge, Model 33A-S11, Boonton Electronics Corp., Morris Plains, N. J.

[21]See, for example, S. M. Sze, *Physics of Semiconductor Devices* (Wiley, New York, 1969), Chap. 9.

[22]A quantitative comparison of the experimental data on InAs with the self-consistent field calculations of Baraff and Appelbaum has been made by G. A. Baraff (unpublished).

[23]The work function is: $\Phi_m = 4.0$ eV for Pb and $\chi = 4.55$ eV for InAs. See, for example, Ref. 21, p. 366; and T. E. Fischer, F. G. Allen, and G. W. Gobeli, Phys. Rev. **163**, 703 (1967).